1

2

3

The coupled dual-oscillator model of wing and haltere motion in flies

5

Tanvi Deora[§] and Sanjay P. Sane*

National Centre for Biological Sciences,

Tata Institute of Fundamental Research,

GKVK Campus, Bellary Road,

Bangalore – 560065

Karnataka, India

*sane@ncbs.res.in

13

14

§ Current address:

Department of Biology,

University of Washington,

Seattle, WA

19

20

21

22

23

24

25

26

Abstract

27

28   The mechanics of Dipteran thorax is dictated by a network of exoskeletal linkages which,

29   when deformed by flight muscles, generate coordinated wing movements. In Diptera,

30   forewings power flight, whereas hindwings have evolved into specialized halteres which

31   provide rapid mechanosensory feedback for flight stabilization. Although actuated by

32   independent muscles, wing-haltere motion is precisely phase-coordinated at high frequencies.

33   Because wingbeat frequency is a product of wing-thorax resonance, wear-and-tear of wings

34   or thorax should impair flight ability. Here, we show that wings and halteres are

35   independently-driven, linked, coupled oscillators. We systematically reduced wing length in

36   flies and observed how wing-haltere synchronization was affected. The wing-wing system is

37   a strongly-coupled oscillator, whereas wing-haltere system is weakly-coupled through

38   mechanical linkages which synchronize phase and frequency. Wing-haltere link is

39   unidirectional; altering wingbeat frequency affects haltere frequency, but not vice-versa.

40   Exoskeletal linkages are thus key morphological features of Dipteran thorax, ensuring robust

41   wing-haltere synchrony despite wing damage.

42

43   Keywords: coupled oscillator, wing coordination, dipteran thorax, wing damage, haltere

44

45

Introduction

Flies are among the best exemplars of aerial agility. The Dipteran order encompasses a vast repertoire of flight types – from the exquisite hovering and maneuvering ability of hoverflies, to the stable trajectories of mosquitoes and rapid territorial chases in houseflies (Land and Collett, 1974). Such complex maneuvers require precise and rapid control, guided by sensory feedback from multiple modalities (Bender and Dickinson, 2006; Heide and Götz, 1996; Hengstenberg, 1993; Pringle, 1948; Sherman and Dickinson, 2003; Trimarchi and Schneiderman, 1995). Of particular importance for flight stability is the mechanosensory feedback from halteres - the modified hind wings of flies - which sense gyroscopic forces during aerial maneuvers (Nalbach, 1993, 1994; Nalbach and Hengstenberg, 1994; Pringle, 1948). During flight, halteres oscillate in a constant plane at frequencies that are identical to their flapping wings, and with a constant relative phase difference. During an aerial turn, an externally imposed change in the plane of haltere oscillation is resisted due to rotational inertia, causing Coriolis torques to act on the haltere base. Mechanical strain in the haltere shaft due to Coriolis torques is sensed by multiple fields of campaniform sensillae distributed around its base. These encode the stroke-by-stroke status of aerial rotations and provide mechanosensory feedback to the wing muscles (Chan and Dickinson, 1996; Fayyazuddin and Dickinson, 1996; Yarger and Fox, 2018). The relative phase difference between the feedback from wing and haltere mechanosensors determines the activity patterns in wing steering muscles (Fayyazuddin and Dickinson, 1999; Fox et al., 2010). During flight, the two wings of flies move exactly in-phase relative to each other, whereas halteres move at a constant phase relative to wings. This precise phase coordination is maintained at wingbeat frequencies that far exceed 100 Hz (Deora et al., 2015; Hall et al., 2015). Because even slight asymmetries in the bilateral wing motions can result in significant instabilities during flight (Fry et al., 2003), the phase and frequency synchronization of the wing-haltere kinematics is a core feature of Dipteran flight, any deviation from which may signal a self-generated aerial turn or an unwanted perturbation.

Previous research has shed much light on the architecture of the Dipteran thorax (Deora et al., 2017; Ennos, 1987; Miyan and Ewing, 1985; Pringle, 1949). The wing-haltere system acts as a complex resonant box. In flies, wings are actuated by two sets of antagonistic indirect flight muscles aligned dorso-longitudinally and dorso-ventrally within the thorax (Deora et al., 2017; Dickinson and Tu, 1997; Pringle, 1949). Their activation is myogenic;

78   hence, contraction in one set of muscles triggers delayed contraction of the other and vice-

79   versa, setting up resonant cycles of oscillations of the entire thorax. A complex wing hinge

80   transforms oscillatory deformations of the thorax into large-amplitude wing strokes. Indirect

81   flight muscles require neural stimulation to remain in an active state, but the frequency of

82   stimulation is typically an order of magnitude lower than resonant thoracic oscillations. The

83   attitude of the wing is finely adjusted on a stroke-to-stroke basis by a set of steering muscles

84   which are under direct neuronal control (Lindsay et al., 2017). Thus, frequency characteristics

85   of Dipteran wing movements are set by the resonance frequency, which in turn is determined

86   primarily by the wing-thoracic morphology. Unlike wings, the motion of each haltere is

87   powered by a single asynchronous muscle whose contractions activate its upstroke, whereas

88   the downstroke is thought to be entirely passive (Pringle, 1949).

89   Although wingbeat frequency depends on wing-thorax morphology, the precise

90   coordination of wings and halteres is mediated by mechanical linkages within the thorax

91   which ensure tight coupling of phase and frequency (Deora et al., 2015). This suggests the

92   hypothesis that wings and halteres act as independent forced oscillators, whose kinematics

93   are both coupled and constrained by two separate mechanical linkages within the thorax (*the*

94   *coupled dual-oscillator hypothesis,* figure 1A). One linkage, *the scutellar link* (alternatively,

95   *wing-wing link*), is embedded within the scutellum and ensures that both wings are

96   synchronized. A second linkage, *the sub-epimeral ridge* (alternatively, *wing-haltere link*),

97   ensures precise coordination of wings and halteres. This linkage ensures only weak-coupling

98   of wing-haltere synchrony, but breaks down when wingbeat frequency exceeds a threshold

99   value (Deora et al., 2015).

100   The resonant properties of such a system rely on mechanical integrity of the wing-

101   thorax system. However, wings of insects often undergo significant natural wear-and-tear

102   during the lifetime of an adult insect (Hayes and Wall, 1999). Wing damage alters both

103   frequency and aerodynamic force generation of the flapping wings (Hedenström et al., 2001),

104   thus posing a challenge to the overall coordination of wing motion. Such damage is typically

105   asymmetric and can affect maneuverability. Not surprisingly, in insects such as bumblebees

106   and dragonflies, wing damage leads to decreased success in hunting and also greater

107   mortality (Cartar, 1992; Combes et al., 2010; Haas and Cartar, 2008).

108   Here, we address two related questions. First, how do flies maintain symmetric wing

109   movement under conditions of wing damage? Second, if wings and haltere motion follows

110   the coupled dual-oscillator hypothesis, how robust are the wing and haltere kinematics in face

111   of wing or thoracic damage? To address these questions, we conducted a series of

112   experiments on the soldier fly, *Hermetia illucens*, in which we made specific lesions of

113   scutellar linkages, and sub-epimeral ridge to impair the mechanical integrity of the thorax. In

114   addition, we either clipped the wings or loaded the halteres to alter their oscillation

115   frequencies. These experiments enabled us to systematically test the predictions of the

116   coupled dual-oscillator hypothesis, and outline the key mechanical properties of the Dipteran

117   thorax that ensure wing-haltere coordination.

Methods

118

i) Surgical treatments and tethering procedure

119

120   1-4 days old soldier flies were cold-anesthetized by placing them in an ice box for 5 minutes.

121   We performed surgical treatments (see figure 1B) before their recovery from cold anesthesia:

122   a) In *Control flies,* no surgeries were performed but they were otherwise handled in the same

123   way as experimental flies.

124   b) In *scutellum-lesioned flies,* we made a small cut only in the scutellum using a scalpel blade

125   (#11, Fine Science Tools Inc., Foster City, CA, USA) while leaving rest of the thorax intact

126   (left panel, figure 1B).

127   c) In *unilateral sub-epimeral ridge lesioned flies,* we lesioned the sub-epimeral ridge at a

128   position anterior to the spiracle on the left side of thorax (middle panel, figure 1B). The right

129   ridge was kept intact and served as internal control. To examine how sub-epimeral ridge

130   influences wingbeat frequency, we compared data from *unilateral sub-epimeral lesioned*

131   group with previously published data on *control* flies (Deora et al., 2015). In both cases,

132   procedures for rearing, handling and tethering were identical.

133   d) In *Bilateral sub-epimeral ridge lesioned flies,* we lesioned sub-epimeral ridges on both

134   sides.

135   e) In *Bilateral haltere ablated flies*, we cut out the knob of halteres on both sides.

136   Post-surgery, we tethered the insects with cyanoacrylate adhesive to the tip of a needle bent

137   to ~90° while they were kept on a pre-chilled metal block. The bent tip provided the

138   necessary surface area to glue a fly to the tether. The tether was lowered using a 3-way

139   micro-manipulator (Narishige Scientific Instrument Laboratory, Tokyo, Japan) and attached

140   dorsally on the scutum of the fly. Flies were given at least an hour for recovery before

141   recording their flight.

ii) Wing-haltere perturbations and filming procedure:

143   We positioned flies at about 60° to the horizontal (approximately its position during free-

144   flight), and elicited flight by lightly touching their abdomen with a brush. We used three

145   high-speed cameras (v7.3 Phantom camera, Vision Research Inc, Wayne, NJ, USA) to film

146   the insects in flight at a resolution of 800x600 pixels at 2000 frames per second

147   (approximately 15-20 times the wingbeat frequency) and 100 μsec exposure. The three

148   cameras (one top view and two side views) captured the 3D motion of both pairs of wings

149   and halteres (figure 1C). The three camera views were calibrated for each filming bout using

150   a custom-made calibration object.

Flies with reduced wing length

152   We first filmed the flight of flies with intact wings, and then switched off the lights to inhibit

153   their flight. Under a dissection microscope attached with a light source and a red-filter to cut

154   off wavelengths below 610 nm, we clipped their wings with a pair of scissors (Fine Science

155   Tools Inc, Foster City, CA, USA) to an appropriate length using wing vein patterns as

156   landmarks. To test the coupled dual-oscillator model (figure 1A), we clipped one wing (either

157   left or right) while keeping the other intact (figure 1B). In all other experiments, both wings

158   were symmetrically reduced. After each round of wing clipping, we filmed the experimental

159   fly in flight. Each series of experiments yielded 4-6 data points including 1 intact and 3-5

160   reduced wing lengths.

Flies with loaded halteres

162   We initially filmed flies with intact wings and halteres, which served as control. Next, we

163   loaded the left haltere with varying amounts of glue and metal shavings under a dissection

164   microscope under red light. Because of the small size of halteres, the amount of load could

165   not be accurately quantified, but we systematically decreased the haltere frequency by

166   incrementing an arbitrary amount of glue and load mixture (right panel, figure 1B). First, we

167   loaded the haltere with glue (Fevicol^{TM} ; polyvinyl acetate, Pidilite Industries) mixed with red

168   poster paint using a metal insect pin. We next added increasing amounts of aluminum

169   shavings mixed with glue and paint to the already loaded haltere. Following each load

170   increment, we filmed the tethered fly. After three rounds of loading, we carefully removed

171   the film of glue, paint and metal shaving with a pair of forceps under the microscope and

172   again filmed the flight recovery. In a few cases, flies removed the load while self-grooming.

173   This experimental procedure yielded 5 data points for each fly – 1 intact, 3 increasing

174   amounts of load and 1 with the load removed.

Results

176   *Asymmetric wing damage does not alter wing coordination*

177   The left and right wings are coupled by a mechanical linkage running through the scutellum

178   within the thorax such that the two wings always flap at constant phase relative to each other

179   (figure 1A) (Deora et al., 2015). However, mechanical coupling of the two wings also implies

180   that their flapping frequencies are identical, and thus alteration in the frequency of one wing

181   should correspondingly alter frequency of the contralateral wing. To test this prediction, we

182   filmed the wing motion of tethered soldier flies in which the length of one wing was

183   sequentially reduced while leaving the other intact. Wingbeat frequency of one-wing clipped

184   fly was determined by sampling 20 arbitrarily chosen wing beats. Even after drastic reduction

185   in the length of one wing by >50% of the original length, the frequency of the clipped and

186   intact wings was always identical (figure 2A left and 2B; for additional data see figure S1,

187   p=0.623; Wilcoxon signed-rank test on the maximum wing difference). Thus, the overall

188   wingbeat frequency is determined by the frequency of the intact wing.

189   *Scutellar integrity is essential for wing coordination*

190   According to the coupled dual-oscillator model, lesioning the scutellum should decouple the

191   frequencies of left and right wings. Accordingly, we severed the scutellar linkage and filmed

192   the flies while again sequentially clipping one wing to reduce its aerodynamic resistance

193   thereby increasing its frequency. This resulted in irregular wing beats in these flies, with

194   frequent mid-stroke pauses and an overall reduction in stroke amplitude. Fourier analysis of

195   the time series of wing motion shows that both wings oscillated at very different frequencies.

196   Thus, unlike the intact scutellum case in which frequency synchronization was robust to wing

197   damage (Fig 2A left panel and Fig 2B), the wings of a scutellum-lesioned fly were decoupled

198   from each other (figure 2A right panel and 2C, additional data in figure S2, p=0.022;

199   Wilcoxon signed-rank test on the maximum wing difference). For example, in the typical

200   case of a scutellum-lesioned fly, the clipped wing flapped at 130 Hz when cut to 50% of its

201   original length, as compared to 85 Hz in the intact wing (figure 2C). Lesioning the scutellum

202   disrupts, and reattaching completely restores the phase coordination between both wings

203   (Deora et al., 2015); thus, scutellar integrity is essential to ensure precise coupling of both

204   phase and frequency of the two wings, and imparts robust synchronization even if one or both

205   wings are slightly damaged or torn. These data show that the two wings are strongly coupled

206   by the scutellar link.

207   *Sub-epimeral ridge weakly couples the frequency of each haltere to its ipsilateral wing*

208   The wing and haltere motion on each side is coupled by a separate thoracic element called the

209   sub-epimeral ridge (figure 1B). A small reduction in wing length resulted in a small increase

210   in wingbeat frequency, and concomitant increase in haltere frequency. However, with further

211   reduction of wing length, wingbeat frequencies exceeded ~150% of the initial values, and

212   halteres failed to keep pace with the wings. In such conditions, haltere frequency dropped

213   closer to their natural frequency suggesting that their coupling was weak (figure 3, control

214   haltere (in blue)) (Deora et al., 2015).

215   We next lesioned the sub-epimeral ridge on the left side while keeping the right side intact as

216   internal control. If sub-epimeral ridge is the main coupling link, then lesioning it should cause

217   the haltere frequency on the lesioned (left) side to be decoupled from the increase in wingbeat

218   frequency due to wing shortening. Our data were consistent with this hypothesis; the control

219   (right) haltere frequency matched the wing frequency more robustly than the lesioned left

220   haltere-wing pair (Fig 3A, p=0.039 for wing-treatment haltere pair and p = 0.657 for wing-

221   control haltere pair, one-sided Wilcoxon signed-rank test at wing length bin = [0.6, 0.7]). Not

222   surprisingly, these data were more variable. In 4 out of the 6 experiments, data were

223   consistent with our hypothesis; the frequency of the haltere on the lesioned (left) side either

224   did not increase at all (representative fly in figure 3B, figure S3 A & B) or was decoupled

225   from the wing even with slight changes in wing length, thus displaying no robustness in the

226   wing-haltere synchrony (figure S3C). In 2 flies, however, wingbeat frequency remained

227   relatively unchanged despite clipping the wings incrementally, and haltere frequency on the

228   lesioned side matched halteres on the control side (figure S3 D & E). Together, these results

229   suggest that the sub-epimeral ridge weakly couples wing and haltere oscillation. Haltere

230   motion can accommodate small to moderate changes in wingbeat frequency but fails if these

231   changes are large.

232

233   *Integrity of the sub-epimeral ridge is essential for resonant oscillation of the thorax*

234   In insects with an intact thorax, clipping the wings increases wingbeat frequency by as much

235   as 90 Hz. In flies with unilaterally-lesioned sub-epimeral ridge, changes in wingbeat

236   frequency were relatively moderate (~60 Hz) after wing shortening (figure 4, data for intact

237   flies from Deora et al., 2015, $p<0.05$, Kruskal-Wallis ANOVA followed by the post hoc

238   Tukey-Kramer multi-comparison test, see supplemental methods for additional details).

239   How does lesioning the sub-epimeral ridge alter wingbeat frequency, in addition to

240   decoupling the wings and halteres? One possibility is that a lesioned ridge disrupts the anti-

241   phase motion of wings and halteres, leading to aberrant haltere feedback to wing steering

242   muscles thereby affecting wingbeat frequency. Alternatively, a lesioned ridge could

243   mechanically disrupt frequencies by acting as a free end that dissipates energy, thereby

244   disrupting the overall resonant mechanics of the thorax.

245   To test for these possibilities, we first lesioned the ridges on both sides. In these flies, the

246   increase in wingbeat frequency was even further restricted (<40 Hz). In another set of flies,

247   we kept both the sub-epimeral ridges intact but ablated both halteres. Ablating halteres alters

248   their feedback but does not mechanically disrupt the thoracic linkage network. Clipping

249   wings of the haltere-ablated flies resulted in significantly elevated wingbeat frequency (by

250   ~90 Hz, figure 4) as compared to flies with both sub-epimeral ridges lesioned ($p <0.05$) but

251   similar to flies with an intact sub-epimeral ridge. This suggests that mechanical integrity of

252   these linkages most likely determines wingbeat frequency. Hence, the mechanical integrity of

253   the entire thoracic linkage system, including both the scutellum and sub-epimeral ridge is

254   essential to maintain the resonant properties of the thorax.

255   *Sub-epimeral ridge is a unidirectional linkage*

256   If the sub-epimeral ridge is bidirectional, then wing frequency should change when haltere

257   frequency is experimentally altered, and vice-versa. Halteres, like wings, are powered by

258   myogenic musculature, and thus changing the haltere mass affects its frequency. To test the

259   hypothesis that sub-epimeral linkage is bidirectional, we loaded halteres with small weights

260   thereby altering their frequency, and measured the effect on wingbeat frequency. Unlike the

261   wing clipping, we could not reduce the haltere mass in discrete steps as it is mostly

262   concentrated at the end knob. Instead, we sequentially loaded each haltere knob with small

263   amounts of glue, thus reducing its frequency in discrete steps (Methods (ii); figure S4 A-C).

264   Small loads did not affect haltere frequency, but as the load increased beyond a threshold,

265   haltere frequency decreased in discrete steps. However, wingbeat frequency remained

266   constant in these experiments (figure 5; for individual fly data see figure SF5A-F, p = 0.014;

267   Wilcoxon signed-rank test for left loaded haltere and wing pair). Thus, the sub-epimeral ridge

268   is a unidirectional link, which couples haltere motion to wing motion but not vice-versa. To

269   rule out the possibility that loading the haltere irreversibly damaged haltere muscles or the

270   sub-epimeral ridge, we detached the load and confirmed that haltere frequency recovered and

271   again matched wingbeat frequency (figure 5; S5).

272

Discussion

274   For stable flight, bilateral wing motion must be precisely coordinated, and halteres must

275   maintain a precise phase difference relative to wings to ensure correct feedback to wing

276   steering muscles (Deora et al., 2015; Fayyazuddin and Dickinson, 1999; Fry et al., 2003).

277   Here, we show that the phase and frequency of wings and haltere motion is mechanically

278   coupled by thoracic linkages, thereby imparting robustness of wing-wing and wing-haltere

279   coordination against damage or wear-and-tear.

Mechanical linkages enable robust frequency-phase output despite asymmetric wing damage

281   Physical damage to the wings of adult insects is irreversible, and potentially deleterious for

282   fitness. Wings of certain insects have flexible costal break or specific venation patterns that

283   prevent wing damage (Mountcastle and Combes, 2014). However, despite such adaptations,

284   insects incur wing damage in the wild due to factors like predation and age (Cartar, 1992;

285   Hayes and Wall, 1999) When one or both wings are damaged, the overall aerodynamic load

286   reduces thereby increasing the frequency of thoracic and wing oscillations (Deora et al.,

287   2015). The linkages described here ensure that the phase and frequency matching between

288   wings and halteres is robust despite significant changes in wingbeat frequency, and hence

289   they may be viewed as evolutionary adaptations that impart robustness to wing motion in

290   case of damage or wear-and-tear.

291   Natural wing damage is typically asymmetric. Shortening one wing by as much as 50% did

292   not significantly alter the resonant frequency of thorax, perhaps because stretch-activation is

293   dictated primarily by the wing with greater aerodynamic load. Importantly, in flies with an

294   intact scutellar linkage, asymmetric changes in wing length did not alter the overall

295   synchrony; wings remained bilaterally coordinated, regardless of their length (figure 2).

296   In bees with symmetric or asymmetric wing damage, wingbeat frequency increases during

297   free flight (Hedenström et al., 2001; Vance and Roberts, 2014), perhaps due to reduced wing

298   inertia. Both bees and flies have similar indirect, asymmetric flight muscle architecture.

299   However, contrary to freely flying bees, in our tethered experiments asymmetric wing

300   damage in flies with intact thorax did not increase wingbeat frequency, indicating that insects

301   actively maintain their wingbeat frequencies. However, lesioning the scutellum completely

302   decoupled the frequencies of the two wings of different lengths; shortened wings oscillated at

303   frequencies up to twice that of the intact wing. These results underscore the importance of the

304   scutellar linkage in ensuring precise coordination between the two wings.

305   *Control of bilateral kinematics by indirect flight muscles*

306   When one wing was shortened and the scutellar link was lesioned, the shortened wing

307   flapped at higher frequency than the intact wing. This shows that the indirect flight muscles

308   on the two sides are, in principle, capable of operating at different frequencies, but are

309   constrained to flap synchronously by the scutellar link. These results are consistent with the

310   idea that indirect flight muscles aid the direct flight muscles in power modulation and

311   kinematic control of wings (Gordon and Dickinson, 2006; Lehmann et al., 2013). In intact

312   flies, power modulation occurs under constraints of equal bilateral wingbeat frequency and

313   phase which leaves open the possibility that amplitude or stroke plane can be modulated by

314   power muscles. For instance, during turns, the two sets of dorso-longitudinal muscles can be

315   differentially activated by their motor neurons (Gordon and Dickinson, 2006; Lehmann et al.,

316   2013), potentially leading to differential power output. Moreover, wing damage results in

317   differential force production on the contralateral sides in hawkmoths (Fernández et al., 2012).

318   Asymmetric wing damage in hawkmoths causes activation delay in the dorso-ventral power

319   muscle, resulting in a voluntary yaw-like maneuver towards the undamaged side, perhaps to

320   compensate for the reduced lift on the damaged side. However, it is important to note that

321   although hawkmoths have indirect flight muscles, they are synchronous and hence under

322   direct neural control. Our results suggest that, like hawkmoths, the indirect, asynchronous

323   flight muscles of flies could also modulate power output of the ipsilateral wing, independent

324   of the contralateral power muscles.

325

326   *Role of sub-epimeral ridge in wing-haltere coordination*

327   The sub-epimeral ridge synchronizes the frequency and phase difference between wings and

328   halteres on each side (figure 3, (Deora et al., 2015)). How would the structural diversity of

329   the thorax and linkages in diverse Diptera influence wing-haltere motion? For example, as

330   compared to the rounded thorax with an almost circular sub-epimeral ridge in blowflies, the

331   thorax of mosquitoes is thinner with an oblong sub-epimeral ridge. Presumably, there is also

332   variation in the material properties and strain transfer across the cuticle. Across flies, there

333   are also differences in their haltere kinematics. For example, blowfly halteres flap exactly

334   antiphase to the wings whereas, for mosquitoes this phase is closer to 0.

335   It is not clear how the precise phase difference is set in these flies, but these parameters are

336   likely the outcome of the variation in the thoracic and linkage anatomy across Diptera and the

337   physics of coupled, driven oscillator system. Indeed, when wing and haltere frequencies are

338   decoupled by loading the haltere (figure 5), the haltere oscillates at an altered phase relative

339   to the wing, even when sub-epimeral ridge is intact (figure S6 & 7). Their frequency, on the

340   other hand, is thought to be determined primarily by the stretch-activation properties of their

341   main driving muscles – the indirect flight muscles for wings, and haltere muscles (or

342   Pringle's muscle) for halteres. Because the sub-epimeral ridge couples haltere frequency to

343   wingbeat frequency, their vibration frequency is fine-tuned by this linkage and the overall

344   thoracic geometry.

345   *Weak coupling properties of the sub-epimeral ridge*

346   The sub-epimeral ridge weakly couples wings and halteres. Its stiffness is limited by its

347   material strength and geometry and it can ensure coordination of wing-haltere frequency

348   close to original frequency. At wingbeat frequencies greater than about 150% of the original

349   frequency, the haltere frequency reverts to a value that is closer or equal to its natural

350   frequency. This behavior is typical of independently driven oscillators, coupled by a

351   mechanical element of finite coupling strength (Strogatz, 1994). Moreover, the sub-epimeral

352   ridge acts in a unidirectional manner (figure 5); moderate changes in wingbeat frequency

353   alter the haltere frequency, but not vice-versa. This may be the outcome of the large

354   difference in the wing and haltere masses (and therefore inertia), and their respective

355   muscles. Our experiments show that the aerodynamic load on the wings determines flapping

356   frequency, and the halteres merely follow.

357   *General implications for other insects with asynchronous muscles*

358   Although our study was focused on Dipteran insects, several implications of this study extend

359   beyond Diptera. Indeed, all insects that possess asynchronous flight muscles must rely on

360   linkages for wing-wing coordination. During buzz pollination in bees and pre-flight thoracic

361   vibrations in beetles the wings are folded even as the flight muscles are active and vibrate the

362   thorax (Esch and Franz, 1991; Leston et al., 1965). Such behaviors suggest the presence of

363   passive mechanical linkages in other insect groups that have asynchronous flight muscles. It

364   is also likely that in many cases, relative coordination between the front and the hind wings

365   are mediated by passive linkages analogous to the sub-epimeral ridge in Diptera. Thoracic

366   linkages may also play a very important role in miniature insects, in which there are fewer

367   muscles groups for higher-level control. Extreme miniaturization in insects of the order

368   Diptera, Hymenoptera and Coleoptera (Polilov, 2015) poses severe physiological and

369   biomechanical constraints on the organism (Polilov, 2012; Sane, 2016). Because smaller

370   wings generate reduced aerodynamic lift, miniature insects must flap at increased frequencies

371   to generate enough lift to stay aloft. In such insects, thoracic linkages are likely to play a key

372   role in mediating synchronization of the wings, while also constraining their degrees of

373   freedom. Small body sizes are associated with rapid wingbeat frequencies, often exceeding

374   100Hz (Dudley, 2000). The key results in this paper show that the thoracic morphology of the

375   fly plays an important role in providing robust wing coordination despite wing damage. How

376   thoracic morphology and material characteristics are adapted for such rapid, coordinated

377   wing movements remains a fascinating question for future studies.

Acknowledgments

Competing Interests

383   The authors declare no competing interests

Author contributions

385   SPS and TD designed the experiments; TD performed experiments and analyzed the data;

386   SPS and TD wrote the paper.

References

394 Bender JA, Dickinson MH. 2006. Comparison of visual and haltere-mediated feedback in the
395   control of body saccades in Drosophila melanogaster. *J Exp Biol* **209**:4597–4606.
396   doi:10.1242/jeb.02583

397 Cartar R V. 1992. Morphological Senescence and Longevity - an Experiment Relating Wing
398   Wear and Life-Span in Foraging Wild Bumble Bees. *J Anim Ecol* **61**:225–231.
399   doi:10.2307/5525

400 Chan WP, Dickinson MH. 1996. Position-specific central projections of mechanosensory
401   neurons on the haltere of the blow fly, Calliphora vicina. *J Comp Neurol* **369**:405–418.
402   doi:10.1002/(sici)1096-9861(19960603)369:3<405::aid-cne6>3.0.co;2-9

403 Combes S, Crall J, Mukherjee S. 2010. Dynamics of animal movement in an ecological
404   context: dragonfly wing damage reduces flight performance and predation success. *Biol*
405   *Lett* **6**:426–429. doi:10.1098/rsbl.2009.0915

406 Deora T, Gundiah N, Sane SP. 2017. Mechanics of the thorax in flies. *J Exp Biol* **220**.
407   doi:10.1242/jeb.128363

408 Deora T, Singh AKAK, Sane SPSPS. 2015. Biomechanical basis of wing and haltere
409   coordination in flies. *Proc Natl Acad Sci* **112**:201412279. doi:10.1073/pnas.1412279112

410 Dickinson MH, Tu MS. 1997. The function of dipteran flight muscle. *Comp Biochem Physiol*
411   *a-Physiology* **116**:223–238. doi:10.1016/s0300-9629(96)00162-4

412 Dudley R. 2000. The Biomechanics of Insect Flight. New Jersey: Princeton University Press.

413 Ennos AR. 1987. A Comparative-Study of the Flight Mechanism of Diptera. *J Exp Biol*
414   **127**:355–372.

415 Esch H, Franz G. 1991. Neural Control of Fibrillar Muscles in Bees During Shivering and
416   Flight. *J Exp Biol* **159**:419–431.

417 Fayyazuddin A, Dickinson MH. 1999. Convergent mechanosensory input structures the firing
418   phase of a steering motor neuron in the blowfly, Calliphora. *J Neurophysiol* **82**:1916–
419   1926.

420 Fayyazuddin A, Dickinson MH. 1996. Haltere afferents provide direct, electrotonic input to a
421   steering motor neuron in the blowfly, Calliphora. *J Neurosci* **16**:5225–5232.

422 Fernández MJ, Springthorpe D, Hedrick TL. 2012. Neuromuscular and biomechanical
423   compensation for wing asymmetry in insect hovering flight. *J Exp Biol* 3631–3638.
424   doi:10.1242/jeb.073627

425   Fox JL, Fairhall AL, Daniel TL. 2010. Encoding properties of haltere neurons enable motion
426   feature detection in a biological gyroscope. *Proc Natl Acad Sci U S A* **107**:3840–3845.
427   doi:10.1073/pnas.0912548107

428   Fry SN, Sayaman R, Dickinson MH. 2003. The Aerodynamics of Free-Flight Maneuvers in
429   Drosophila. *Science (80-)* **300**:495–498.

430   Gordon S, Dickinson MH. 2006. Role of calcium in the regulation of mechanical power in
431   insect flight. *Proc Natl Acad Sci* **103**:4311–4315.

432   Haas CA, Cartar R V. 2008. Robust flight performance of bumble bees with artificially
433   induced wing wear. *Can J Zool* **86**:668–675. doi:10.1139/Z08-034

434   Hall JM, McLoughlin DP, Kathman ND, Yarger AM, Mureli S, Fox JL. 2015. Kinematic
435   diversity suggests expanded roles for fly halteres. *Biol Lett* **11**:20150845.
436   doi:10.1098/rsbl.2015.0845

437   Hayes EJ, Wall R. 1999. Age-grading adult insects: A review of techniques. *Physiol Entomol*
438   **24**:1–10. doi:10.1046/j.1365-3032.1999.00104.x

439   Hedenström A, Ellington CP, Wolf TJ. 2001. Wing wear, aerodynamics and flight energetics
440   in bumblebees (Bombus terrestris): An experimental study. *Funct Ecol* **15**:417–422.
441   doi:10.1046/j.0269-8463.2001.00531.x

442   Heide G, Götz KG. 1996. Optomotor Control of Course and Altitude in Drosophila
443   Melanogaster is Correlated with Distinct Activities of at Least Three Pairs of Flight
444   Steering Msucles. *J Exp Biol* **1726**:1711–1726.

445   Hengstenberg R. 1993. Multisensory control in insect oculomotor systems. *Rev Oculomot Res*
446   **5**:285–98.

447   Land M, Collett T. 1974. Chasing Behaviour of Houseflies (Fannia canicularis). *J Comp*
448   *Physiol* **331**–**357**.

449   Lehmann F, Skandalis DA, Berthé R. 2013. Calcium signalling indicates bilateral power
450   balancing in the Drosophila flight muscle during manoeuvring flight. *J R Soc Interface*
451   **10**.

452   Leston BYD, Pringle JWS, White DC. 1965. Muscular Activity During Preparation For
453   Flight in a Beetle. *J Exp Biol* **42**:409–414.

454   Lindsay T, Sustar A, Dickinson M. 2017. The Function and Organization of the Motor
455   System Controlling Flight Maneuvers in Flies. *Curr Biol* **27**:345–358.
456   doi:10.1016/j.cub.2016.12.018

457   Miyan JA, Ewing AW. 1985. How Diptera move their wings - A re-examination of the Wing
458   Base Articulation and Muscle Systems Concerned with Flight. *Philos Trans R Soc*
459   *London Ser B-Biological Sci* **311**:271–302. doi:10.1098/rstb.1985.0154

460   Mountcastle AM, Combes SA. 2014. Biomechanical strategies for mitigating collision
461   damage in insect wings: structural design versus embedded elastic materials. *J Exp Biol*
462   **217**:1108–1115. doi:10.1242/jeb.092916

463   Nalbach G. 1994. Extremely Nonorthogonal Axes in a Sense Organ for Rotation -
464   Behavioral-Analysis of the Dipteran Haltere System. *Neuroscience* **61**:149–163.
465   doi:10.1016/0306-4522(94)90068-x

466   Nalbach G. 1993. The Halteres of the Blowfly Calliphora .1. Kinematics and Dynamics. *J*

467   *Comp Physiol a-Sensory Neural Behav Physiol* **173**:293–300. doi:10.1007/bf00212693

468   Nalbach G, Hengstenberg R. 1994. The halteres of the blowfly Calliphora II. Three-
469   dimensional organization of compensatory reactions to real and simulated rotations. *J*
470   *Comp Physiol* **175**:695–708.

471   Polilov AA. 2015. Small Is Beautiful: Features of the Smallest Insects and Limits to
472   Miniaturization. *Annu Rev Entomol* **60**:103–121. doi:10.1146/annurev-ento-010814-
473   020924

474   Polilov AA. 2012. The smallest insects evolve anucleate neurons. *Arthropod Struct Dev*
475   **41**:29–34. doi:10.1016/j.asd.2011.09.001

476   Pringle JWS. 1949. The Excitation And Contraction Of The Flight Muscles Of Insects. *J*
477   *Physiol* **108**:226–232.

478   Pringle JWS. 1948. The Gyroscopic Mechanism Of The Halteres Of Diptera. *Philos Trans R*
479   *Soc London Ser B-Biological Sci* **233**:347–384. doi:10.1098/rstb.1948.0007

480   Sane SP. 2016. Neurobiology and biomechanics of flight in miniature insects. *Curr Opin*
481   *Neurobiol* **41**:158–166.

482   Sherman A, Dickinson MH. 2003. A comparison of visual and haltere-mediated equilibrium
483   reflexes in the fruit fly Drosophila melanogaster. *J Exp Biol* **206**:295–302.
484   doi:10.1242/jeb.00075

485   Strogatz SH. 1994. Non-linear Dynamics and Chaos. New York: Perseus Books.

486   Trimarchi JR, Schneiderman AM. 1995. Different neural pathways coordinate Drosophila
487   flight initiations evoked by visual and olfactory stimuli. *J Exp Biol* **198**:1099–1104.

488   Vance JT, Roberts SP. 2014. The effects of artificial wing wear on the flight capacity of the
489   honey bee Apis mellifera. *J Insect Physiol* **65**:27–36.
490   doi:10.1016/j.jinsphys.2014.04.003

491   Yarger AM, Fox JL. 2018. Single mechanosensory neurons encode lateral displacements
492   using precise spike timing and thresholds. *Proc R Soc B Biol Sci* **285**.
493   doi:10.1098/rspb.2018.1759

494

Figure legends

496   **Figure 1: The experimental setup.** (A) Schematic of a tethered fly showing the position of

497   the three high-speed cameras. Insets show the three different camera views. (B) Mechanical

498   model of the Dipteran thorax modified from an earlier work (Deora et al., 2015). This model

499   excludes the clutch and gearbox from the previous figure, focusing instead on the wing-wing

500   and wing-haltere linkages which are the main focus of the experiments described here. (C) A

501   schematic (top) and model (bottom) illustrating the experimental treatments. The treatments

502   (red) included lesioning the scutellum or wing-wing link (left panel), lesioning sub-epimeral

503   ridge or wing-haltere link (middle panel) and haltere-loading (right panel). The clipped wings

504   are also indicated (dotted lines). The same treatments are also shown in the model schematic,

505   and used as insets in later figures.

506   **Figure 2: The frequency of the two wings is synchronized by the scutellum.** (A)

507   Wingbeat frequency of intact (grey) and clipped (red) wing as a function of clipped-wing

508   length for intact thorax (left panel) and slit scutellum (right panel). Flies with intact thorax

509   flap their wings at identical frequencies whereas the *scutellum-lesioned* flies' flap at different

510   frequencies. Each dot represents an individual fly. (B) Wingbeat frequency as a function of

511   clipped wing length for a representative, intact fly plotted as compact box plot (~20

512   wingbeats are analyzed at each wing length). (C) Peak wingbeat frequency as a function of

513   clipped wing length for a representative *scutellum-lesioned* fly. Insets show schematic for

514   treatments. Additional data for individual flies can also be found in SF 1 and 2.

515   **Figure 3: Sub-epimeral ridge couples the frequency of wings and halteres.** Frequency of

516   wing (grey), control haltere (blue) and haltere with the sub-epimeral ridge lesioned (red) as a

517   function of wing length across all flies (A) and one representative fly (B). Inset shows the

518   schematic for treatments. Additional data for individual flies can be found in SF3.

519   **Figure 4: Sub-epimeral ridge lesions alter the resonant properties of the thorax.**

520   Individual box plots show increase in wing beat frequency for reduced wing length in

521   different treatment groups. Flies with one or both sub-epimeral ridge lesioned show a smaller

522   increase in wing beat frequency as compared to intact flies. In contrast, flies with both haltere

523   ablated can increase their wing beat frequency significantly more than flies with both sub-

524   epimeral ridges lesioned. (* p value < 0.05, non-parametric Kruskal-Wallis ANOVA

525   followed by a Tukey-Kramer post hoc multi-comparison test, n; 8 intact flies, 6 flies for the

526   other three treatments). Insets under each group show the schematic for treatments.

527   **Figure 5: Wing-haltere linkage is unidirectional because changing haltere frequency**

528   **does not alter wingbeat frequency.** Frequency of wing (grey), control haltere (blue) and

529   loaded haltere (red) across all flies. Each dot represents a single individual fly. The haltere

530   frequency drops as the haltere is loaded but the wing frequency remains the same showing

531   that wing-haltere coupling is unidirectional. Inset shows the schematic for the treatment. Data

532   for individual flies can be found in SF5. (B) Representative images of the haltere loaded with

533   different amounts of load (also see figure S4).

17
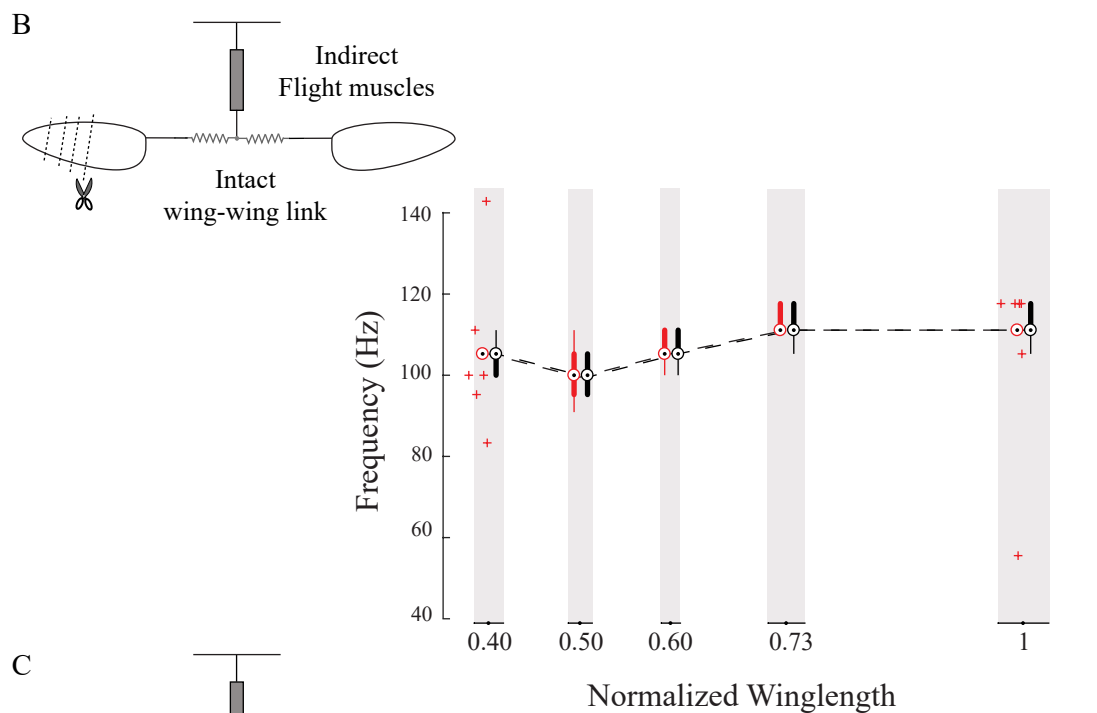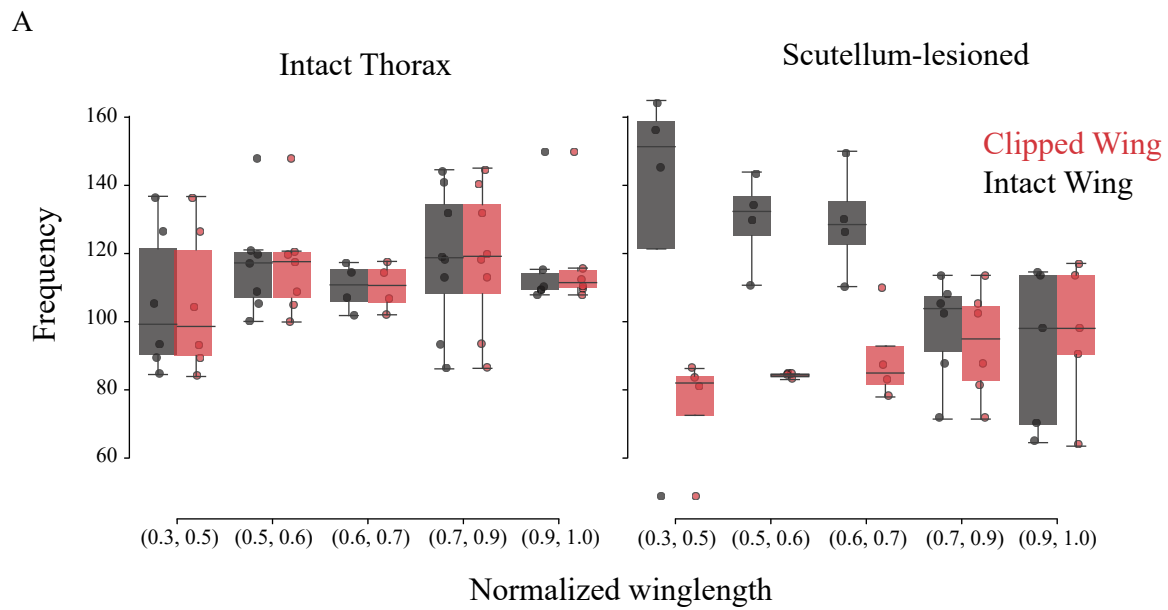
A

B

C

A

Intact Thorax · Scutellum-lesioned

Clipped Wing · Intact Wing
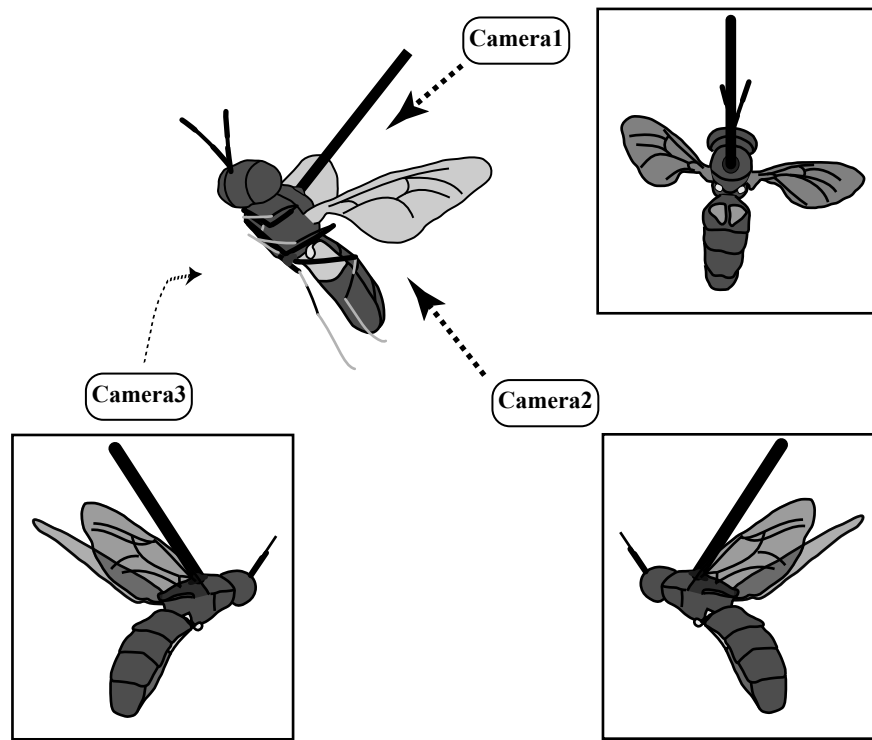
B
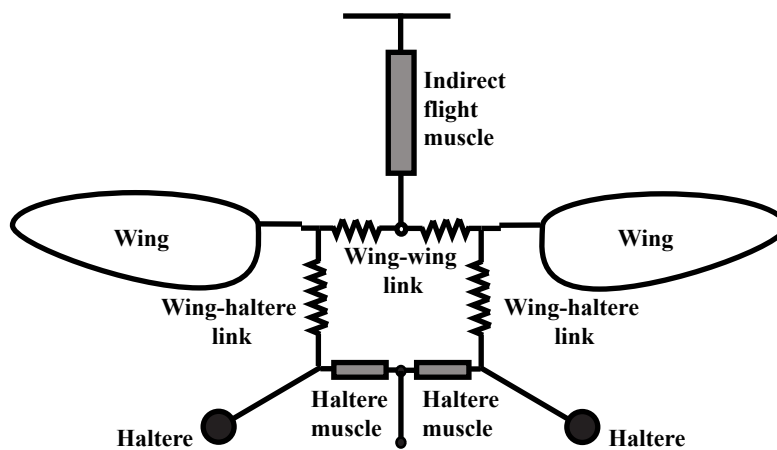
C
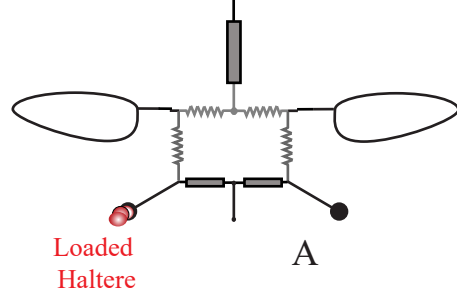
Deora and Sane
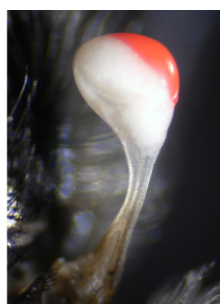**Figure 4**

Deora and Sane
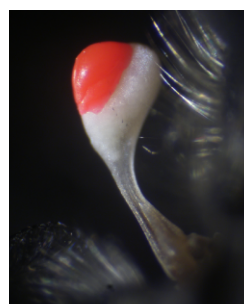**Figure 5**

Loaded
Haltere

A
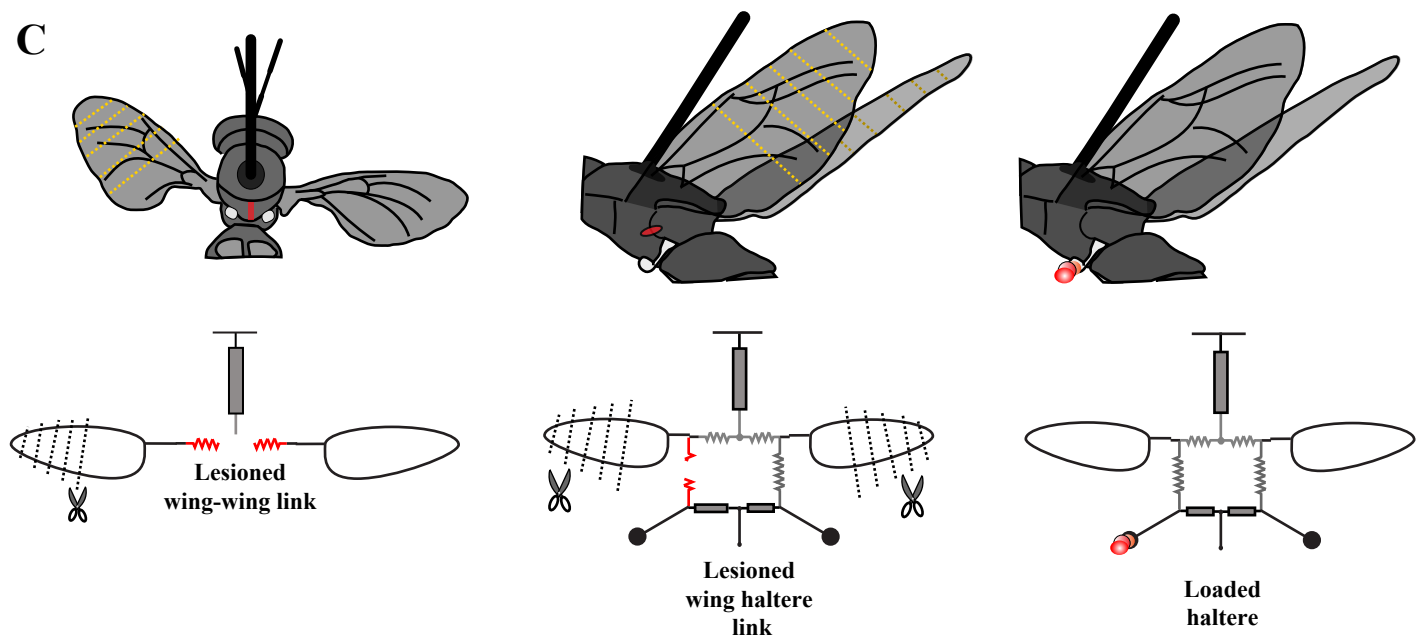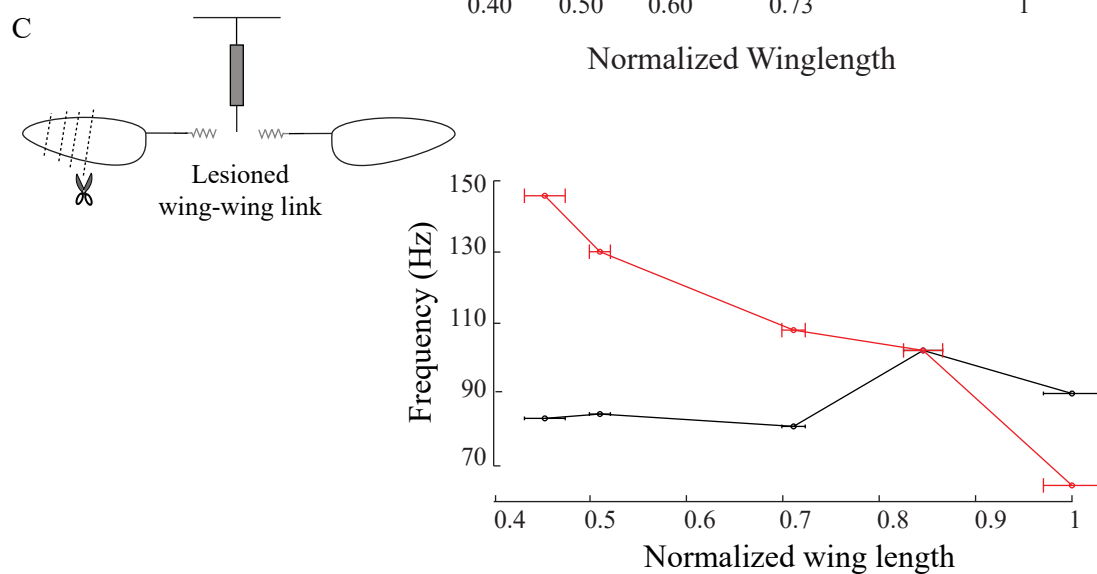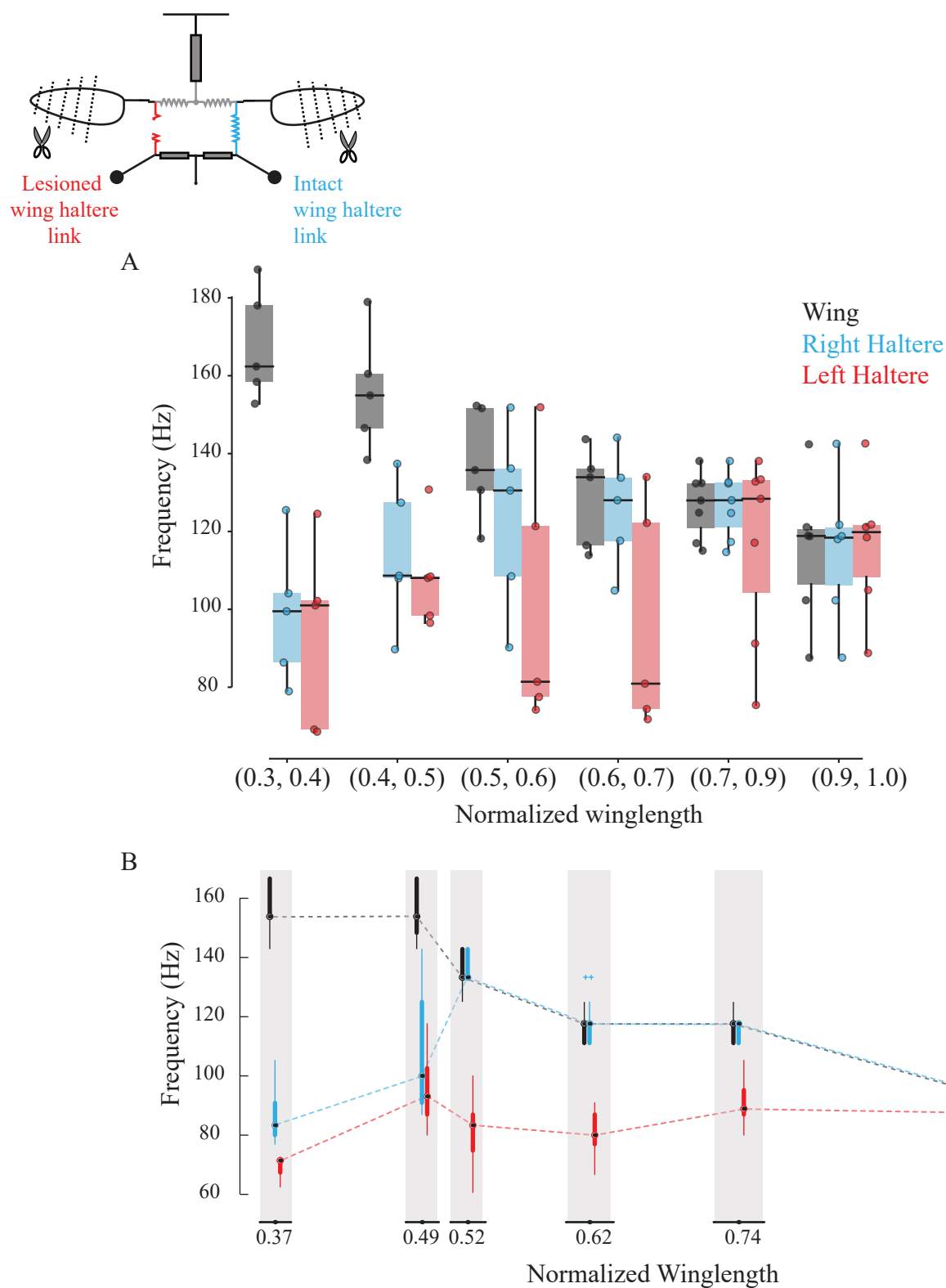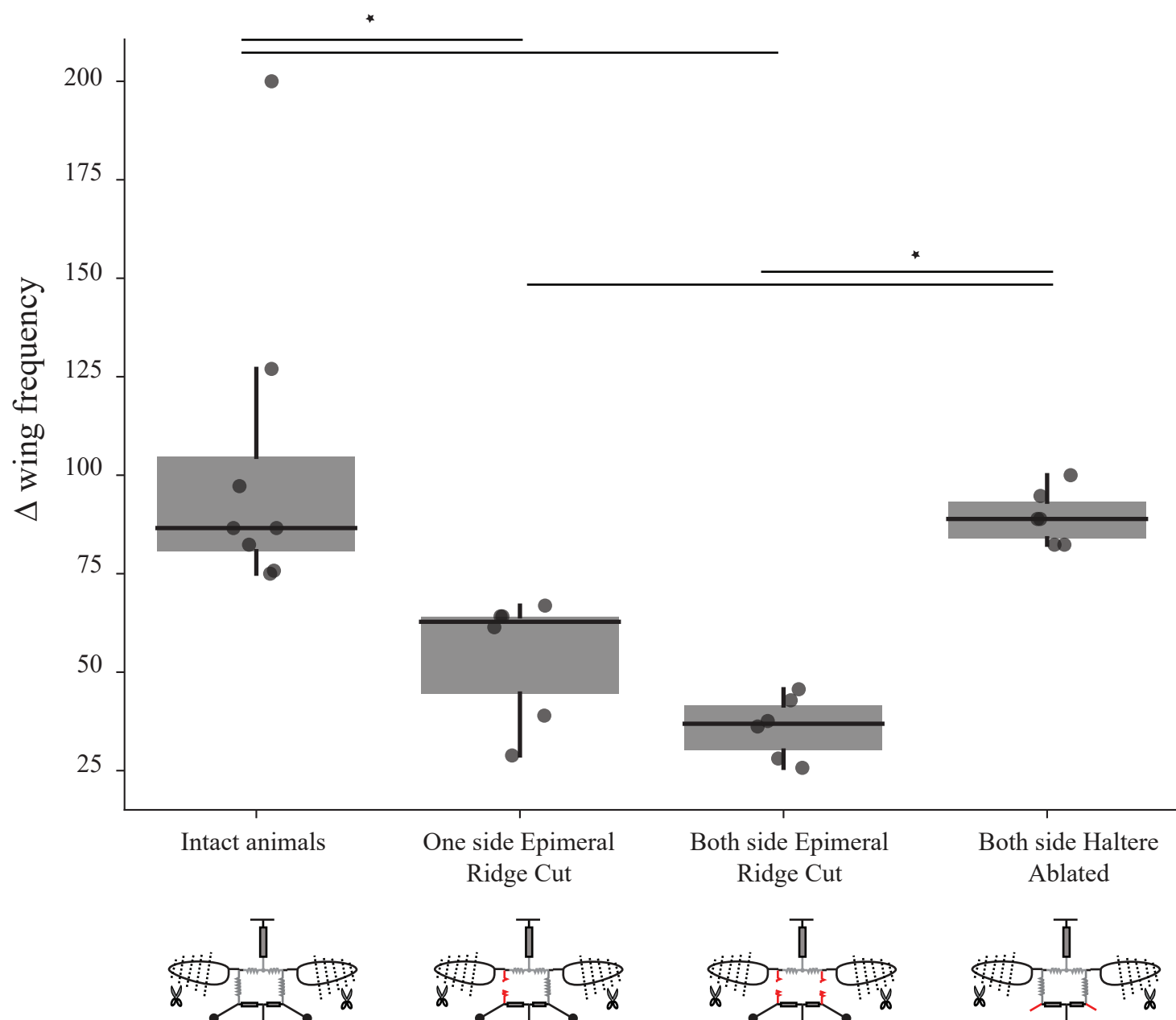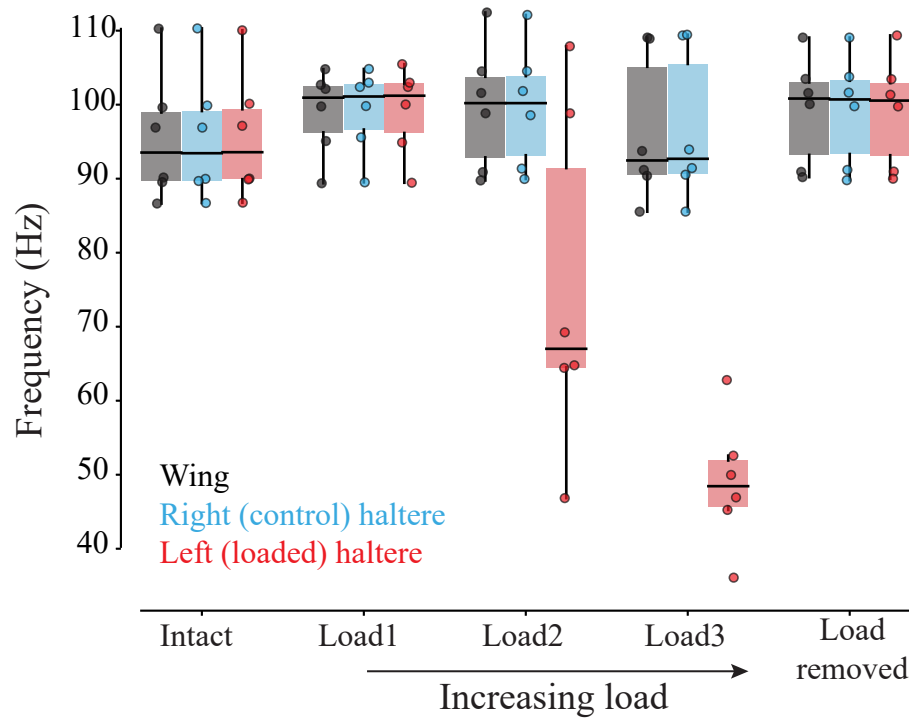
B

Load 1:
Only paint

Load 2:
Paint and
small metal
piece

Load 3:
Paint and
large metal
piece

Supplementary Material

The coupled dual-oscillator model of wing and haltere coordination in flies

Methods:

i) Soldier fly rearing procedure:

Wild caught black soldier flies, *Hermetia illucens* were enclosed in vials filled with a medium of corn flour and agar mixed with yeast powder. In most cases, we caught wild gravid females which laid eggs immediately upon capture. We reared the larvae on the artificial medium, frequently replacing it as the larvae grew. Through most of the year, adult flies emerged approximately a month after pupation, but their emergence during winters could be more delayed due to diapause. Adult soldier flies were maintained in mesh cages on a 12:12 hour day-night cycle. Some flies were reared on compost in which wild gravid females laid eggs. The larvae fed and pupated in the compost. Pupae were separated and collected in a separate box. Adults were maintained in natural day-night cycle. Animals reared in this manner were typically bigger and more active than lab-reared animals but showed no difference in behavior.

ii) Analysis:

We computed the time period (and frequency) of a single wing and haltere stroke from videos by counting the number of frames per wing stroke. We analyzed 20 strokes per flight bout at each wing length. In the *scutellum-lesioned group,* the flies often flapped their wings with varying amplitude and frequency making it difficult to ascertain the precise time duration for each wing stroke. We digitized the videos of these animals using the DLTdv3 code (Hedrick, [1]) in MATLAB (Mathworks Inc, Natick, MA, USA) and analyzed the data using custom MATLAB codes. For each wing, we calculated the azimuthal (theta) angle and plotted the theta position of both wings as a function of time and obtained the average wing beat frequency using Fourier analysis.

We calculated the change in wingbeat frequency after clipping wing length (ΔF), as

$$\Delta F_s = F_S - F_i$$

where,

F_s = wing beat frequency at the shortest wing length

F_i = wing beat frequency at the intact wing length

Increment in wingbeat frequency due to reduced wing length (ΔF) for all four groups was compared using non-parametric Kruskal-Wallis ANOVA followed by the Tukey-Kramer post hoc multi comparison analysis. Codes used for analysis can be found at https://github.com/TanviDeora/Coupled_Dual-oscillator_DeoraSane.

References

1. Hedrick TL. 2008 Software techniques for two- and three-dimensional kinematic measurements of biological and biomimetic systems. *Bioinspir. Biomim.* **3**. (doi:10.1088/1748-3182/3/3/034001)

Table 1: p values for a one-sided Wilcoxon signed rank sum test at all wing length bins for epimeral ridge cut flies in Figure 3A.

Wing length bin	Epimeral Ridge Cut Haltere -wing	Control Haltere – wing
(0.9, 1.0)	0.962632	0.553631
(0.7, 0.9)	0.458256	0.541744
(0.6, 0.7)	0.039808	0.657085
(0.5, 0.6)	0.039808	0.250092
(0.4, 0.5)	0.021557	0.021557
(0.3, 0.4)	0.021557	0.021557

Table 2: p values for a one-sided Wilcoxon signed rank sum test between haltere and wing pairs at all haltere loads in Figure 5.

	Loaded Haltere - wing	Control Haltere - wing
Intact haltere	0.875568	0.827384
Load 1	0.963031	0.986146
Load 2	0.013854	0.662929
Load 3	0.013854	0.986146
Load removed	0.231536	0.342915

Testing Significance and estimating sample sizes:

To estimate a minimum sample size to detect a difference between two groups, we used the estimated mean and std of these two groups (measured from data) and simulated datasets of different sample sizes. For each simulated dataset, we calculated the p value using the relevant test (Wilcoxon signed-rank test for all paired data and Kruskalwallis for groups). We used a bootstrapping method; repeating this about 10,000 times for each sample size and estimated the power, i.e. probability of detecting a difference between these two groups at significance level of 0.05. Below we report the tested groups and power analysis for each experiment.

Wing Coordination by Scutellum (Figure 2)
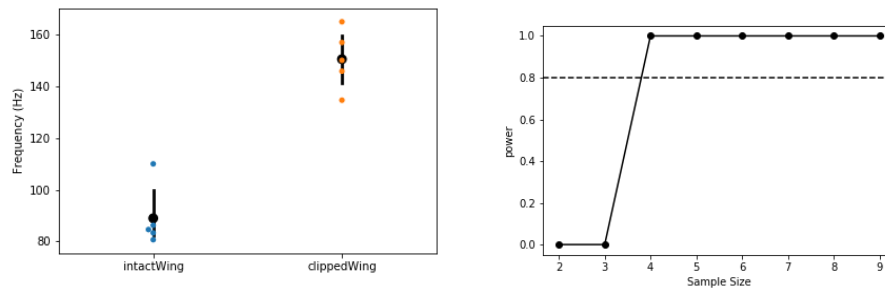
(*Left*) The frequency of intact and clipped wing (at the wing length which has the largest difference) are significantly different (Wilcoxon signed-rank test, p = 0.021). (*Right*) Power analysis for different sample sizes. Our sample size of 6 is greater than the minimum sample size (=4) needed to have 80% confidence level (dashed line)

Wing-Haltere Coordination by Epimeral Ridge (Figure 3)
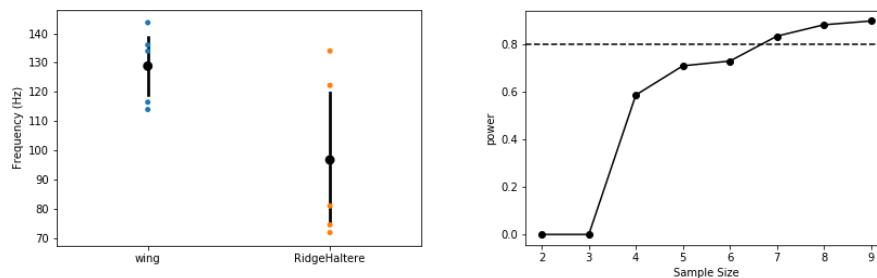
(*Left*) The frequency of wing and epimeral ridge cut haltere at wing length bin of (06 - 0.7) which has the largest difference) are significantly different (Wilcoxon signed-rank test, p = 0.039). (*Right*) Power analysis for different sample sizes. At our current sample size, we have a power of 0.713 that is we have a 71.3 % chance of picking up a significant difference.

**Integrity of Epimeral Ridge and Thoracic Resonance (Figure 4)**

For one-way Kruskal Wallis test, our sample size, n = 8 for control and 6 for the 3 treatments groups each. We used a similar bootstrapping method, simulating our data based on our group mean and std, and calculating the power at difference sample sizes. To detect a significant difference at 80% chance we require a minimum of 9 samples. With our current sample size (n = 6), we have a substantial Type II error: that is a 48% chance of not detecting a difference if they were indeed different.
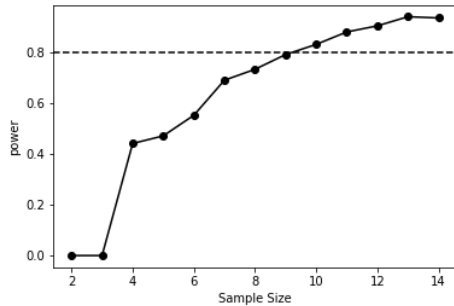
Loading Haltere (Figure 5)
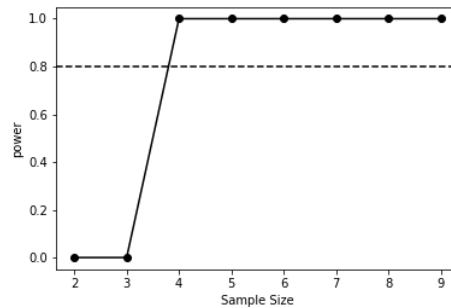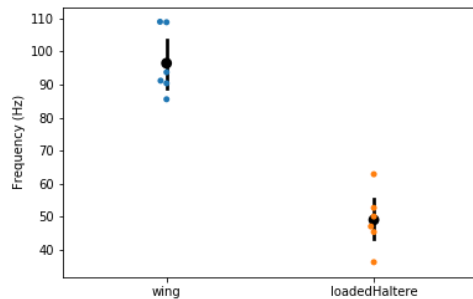
(*Left*) The frequency of wing and loaded haltere at maximum loading ("load3") are significantly different (Wilcoxon signed-rank test (p =0.013). (*Right*) Power analysis for different sample sizes. Our sample size of 6 is greater than the minimum sample size (=4) needed to have 80% confidence level (dashed line)
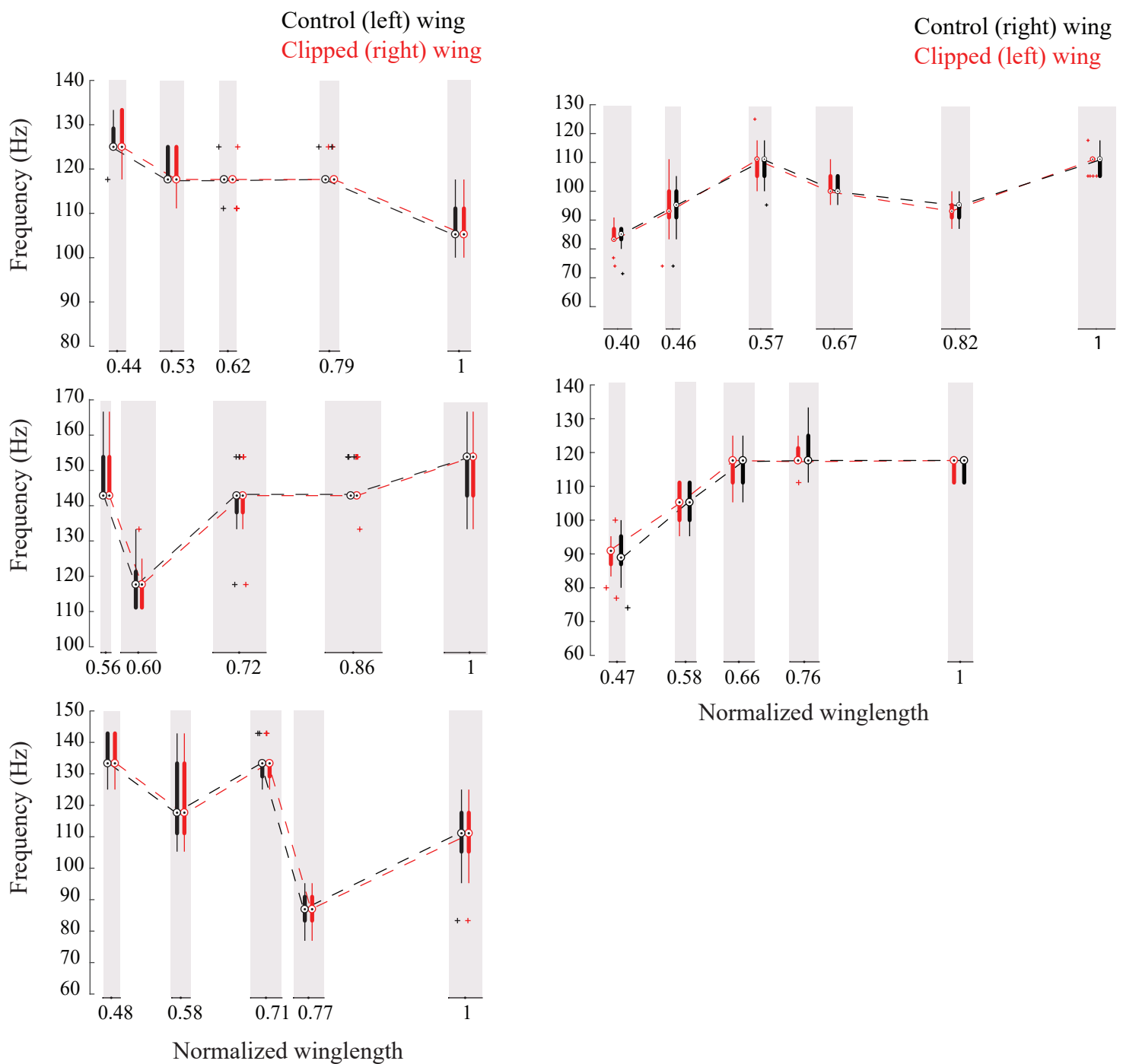
Supplementary Figure 1: The frequencies of the two wings are coupled. Frequency of the intact (black) and clipped (red) wing plotted as compact box plot as a function of the clipped wing length for five individual flies showing that flies always flap the wings at the same frequency.
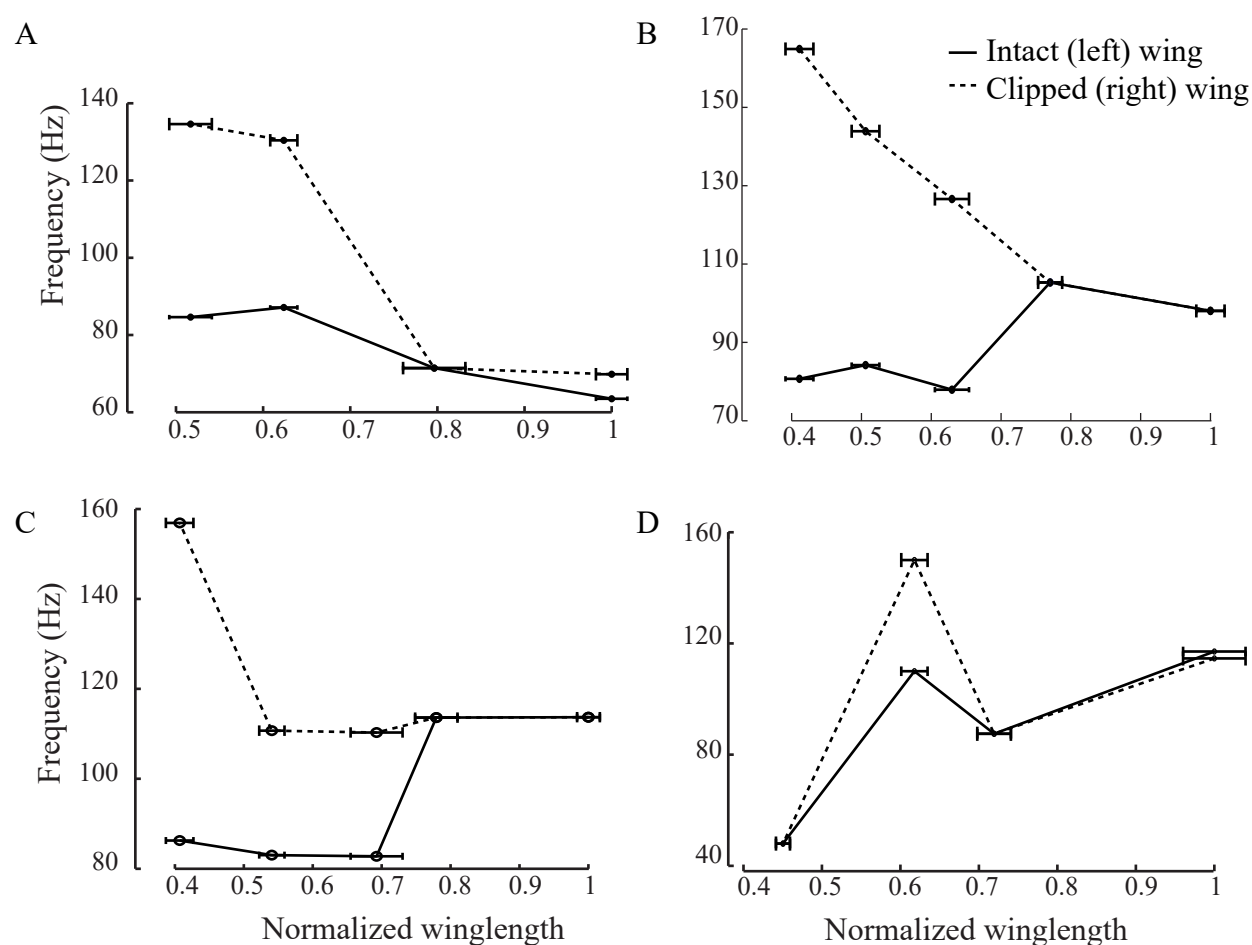
Supplementary Figure 2: Scutellum synchronizes the frequencies of the two wings. Individual plots show the peak wing beat frequency for intact (black solid) and clipped (black dotted) wing as a function of the clipped wing length for four individual flies showing that the scutellum-lesioned flies flap their wings at different frequencies.
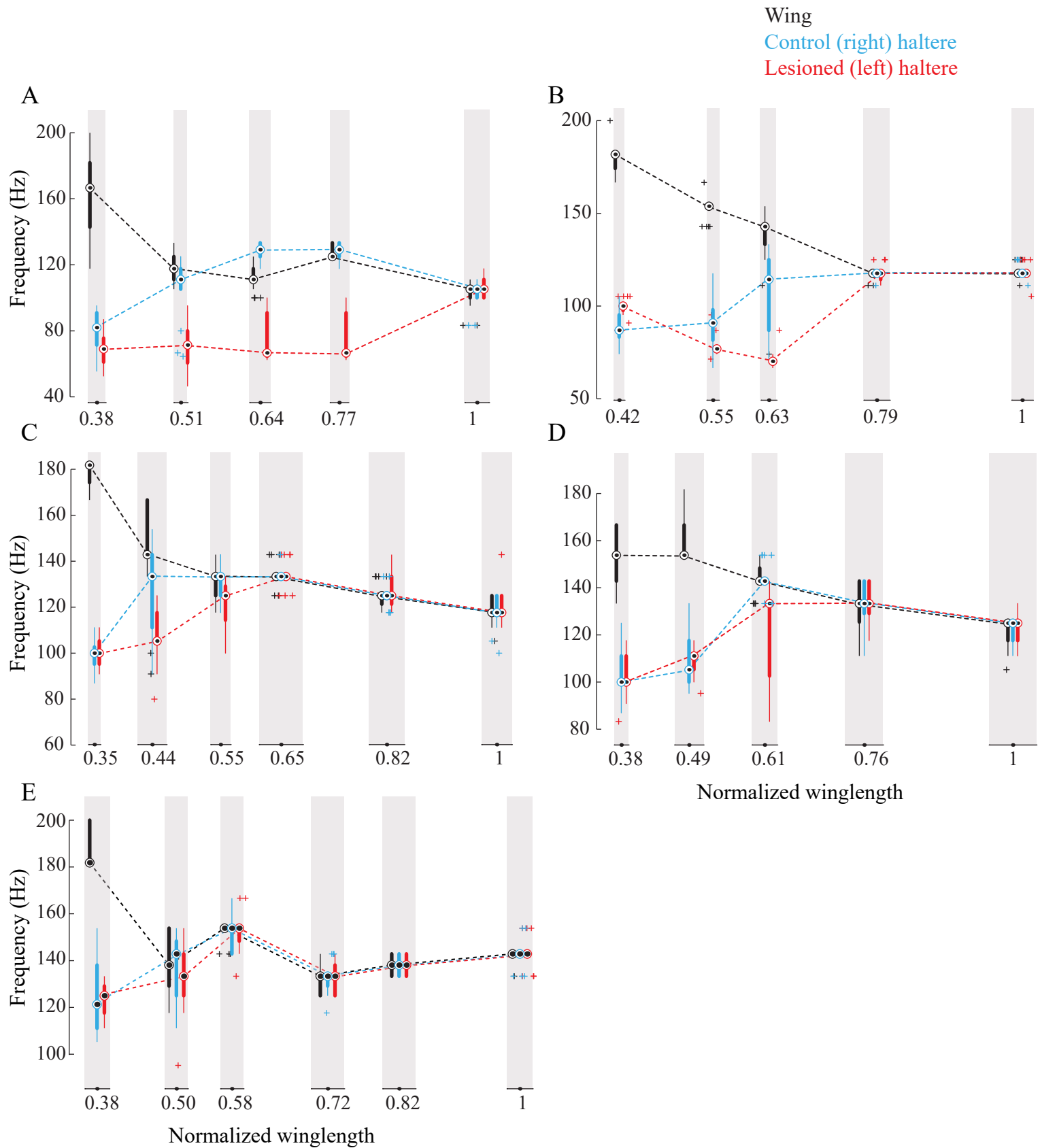
Supplementary Figure 3: Sub-epimeral ridge couples the frequency of wings and halteres. (A-E) Frequency of wing (black), control haltere (blue) and haltere with the sub-epimeral ridge lesioned (red) plotted as compact box plot as a function of wing length for five individual flies.
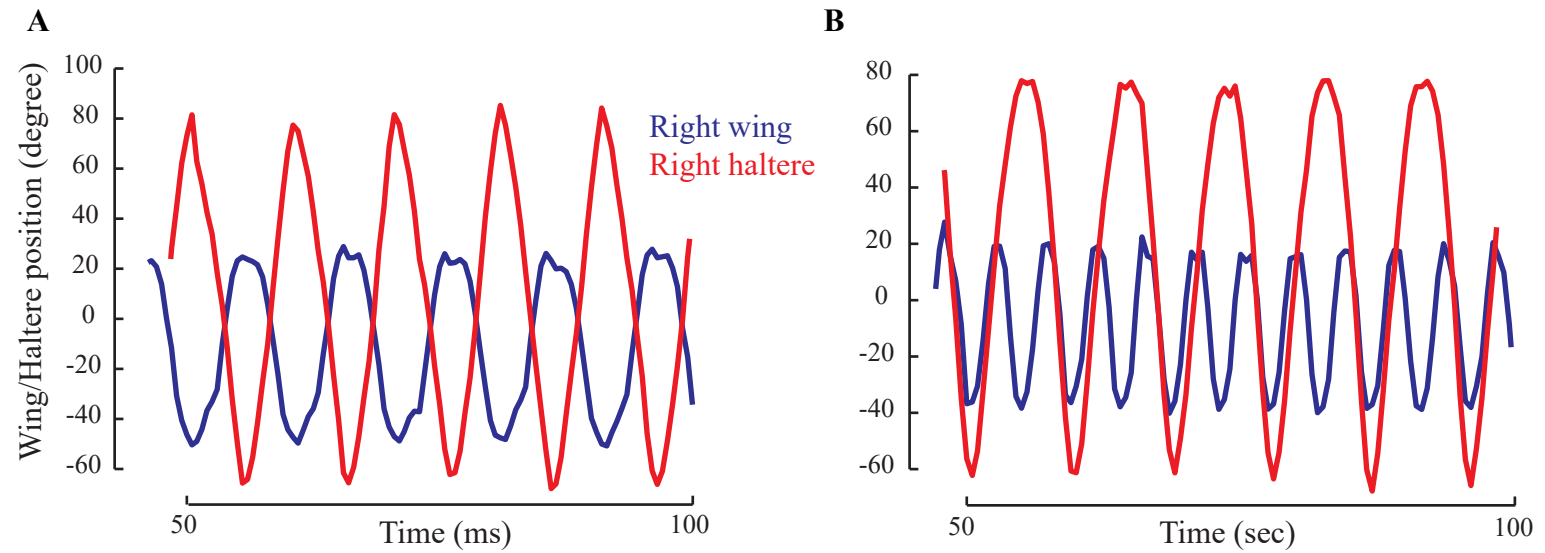
Deora and Sane

Supplementary Figure 4
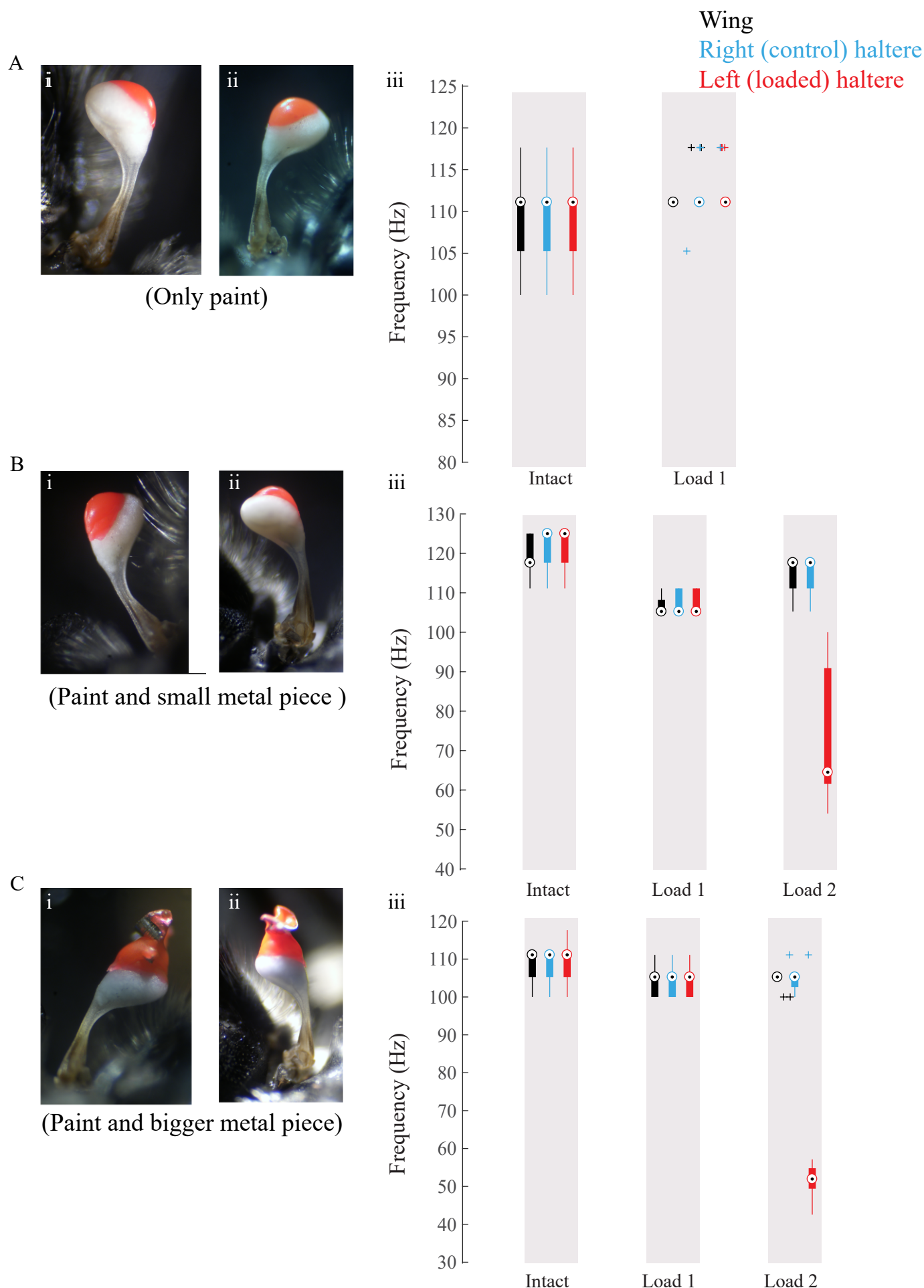
Supplementary Figure 4: Increasing amounts of glue, paint and metal shavings were added to load halteres (A-C) Data for individual flies showing loaded haltere (load visible in red) in the dorsal (i) and ventral (ii) views and the corresponding wing (black), control right haltere (blue) and loaded left haltere (red) frequency.
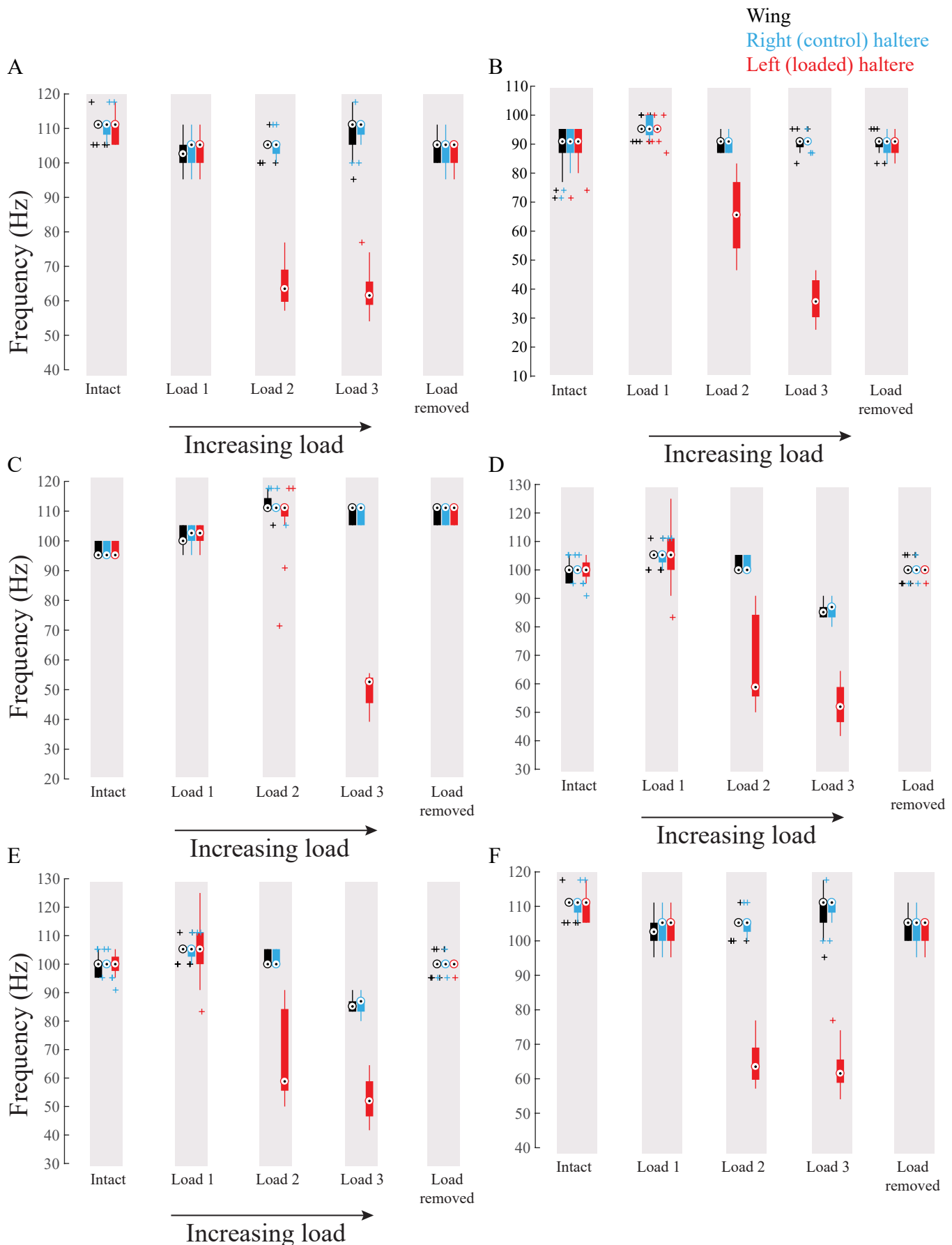
Supplementary Figure 5: Wing haltere coupling acts unidirectionally such that changing haltere frequency does not influence wing frequency. (A-F) Frequency of wing (black), control haltere (blue) and loaded haltere (red) plotted as compact box plot for five individual flies. The haltere frequency drops as the haltere is loaded but the wing the frequency remains the same showing that wings and halteres coupling works in a unidirectional manner.

Supplementary Figure 6: The positions of wing (blue) and haltere (red) showing their relative phase for a representative fly with intact wings (A) and wings cut (B). (A) When the wing and haltere frequencies are matched, they are perfectly antiphase. (B) However, when the beat frequency increases, the haltere cycles through different phases relative to the wing.
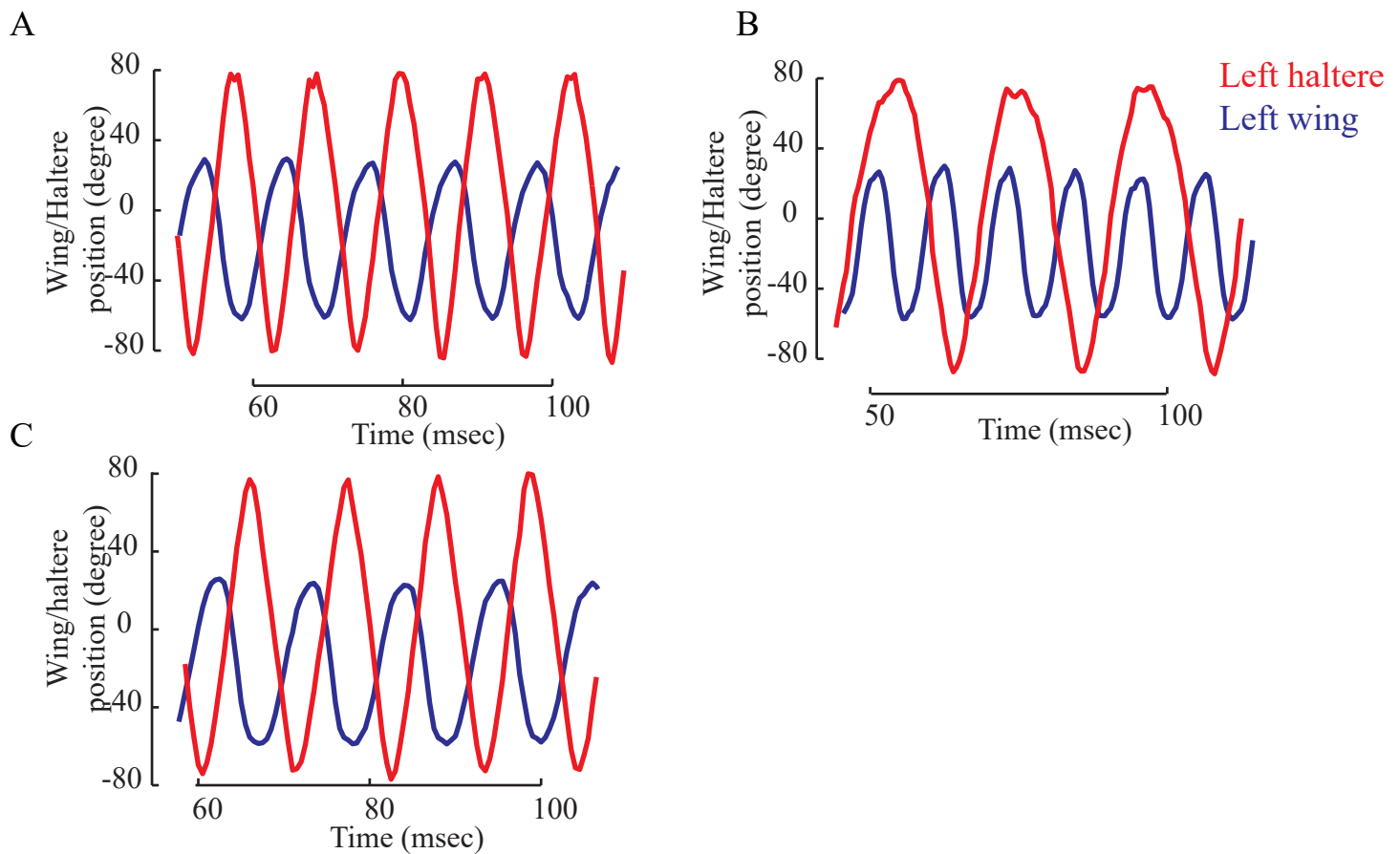
Supplementary Figure 7: The wing (blue) and haltere (red) position showing their relative phase for a representative fly with intact halteres (A), loaded halteres (B) and the load removed (C). (A) The wing and haltere oscillate antiphase when their frequencies matches (A and C), but haltere cycles through different phases relative to the wing when the haltere frequency drops.